Vol 18 No 4, April 2009
1674-1056/2009/18(04)/1631-06

Chinese Physics B

© 2009 Chin. Phys. Soc.
and IOP Publishing Ltd

Study on reaction mechanism of $YBa_2Cu_3O_{7-x}$ film by TFA-MOD process*

Ding Fa-Zhu(丁发柱)[a)†], Lü Xu-Dong(吕旭东)[a)], Gu Hong-Wei(古宏伟)[a)‡], Li Tao(李 弢)[a)], and Cao Jiang-Li(曹江利)[b)]

[a)] *Superconductor Research Center, General Research Institute for Non-ferrous Metals, Beijing* 100088, *China*

[b)] *School of Materials Science and Engineering, University of Science and Technology Beijing, Beijing* 100083, *China*

(Received 2 July 2008; revised manuscript received 7 November 2008)

This paper systematically investigates the intermediate phases of $YBa_2Cu_3O_{7-x}$ (YBCO) film prepared by metalorganic deposition method using trifluoroacetates (TFA-MOD). According to x-ray diffraction and Raman analyses, the precursor film decomposed in a mixture of BaF_2, Y_2O_3 and CuO after the pyrolysis process. Then these intermediate phases converted into tetragonal $YBa_2Cu_3O_{6.5}$ at about 725 °C. The influence of water vapour pressure on the $YBa_2Cu_3O_{7-x}$ film growth on $LaAlO_3$ single-crystal substrates was also studied. The films prepared at low water vapour pressures (40–140 hPa) showed poor electrical performance due to the *a*-axis grain structure and impurity phases. However, the films prepared at 190 hPa exhibited the highest critical temperature of 90 K and the highest J_c of 3.8 MA/cm^2, which was attributed to the formation of a purer YBCO phase and stronger biaxial texture.

Keywords: TFA-MOD, YBCO, intermediate phase, water vapour pressure
PACC: 7470V, 7475, 8115

1. Introduction

The $YBa_2Cu_3O_{7-x}$ (YBCO) is currently the most researched materials for second-generation superconducting wire, and hopefully the best candidate materials for wires requiring high critical current density up to MA/cm^2 at 77 K. Thus, in the development of second-generation wires, a primary concern is choosing a cost-effective manufacturing process that maintains high electrical performance in the YBCO film. Among various processes used for the deposition of YBCO films,[1−6] trifluoroacetate (TFA-MOD) is a promising approach for its valuable advantages such as composition adjustability and low cost. Recently, many research groups have fabricated high quality YBCO films by TFA-MOD process.[7−16] However, nowadays the intermediate phases proposed to obtain YBCO film by TFA-MOD method remain controversial and are poorly understood. In previous studies, Smith *et al*[17] reported that the intermediate phases are $Y_2Cu_2O_5$, BaF_2 and CuO, based on their investigations of YBCO films grown on $LaAlO_3$ (LAO) single crystals. On the other hand, Araki *et al*[9] proposed the intermediate phases of CuO and Y-Ba-O-F from their investigations using transmission electron microscopy (TEM) and x-ray diffraction (XRD). In addition, Wu *et al*[18] suggested the intermediate phases of Cu_2O and Y–Ba–O–F based on their studies on YBCO films grown onto $SrTiO_3$ substrates. Although the proposed intermediate phases are different, they are finally transformed into YBCO after reacting with water during the firing process. In these reactions, the water vapour pressure is a key factor to control the supersaturation which determines the growth rate of the YBCO conversion kinetics. Epitaxial growth of YBCO films proceeds through a solid–gas chemical reaction involving transport of H_2O gas to the growing interface and the corresponding outward HF diffusion. Moreover, critical currents of YBCO films are sensitive to the $P(H_2O)$.[12] Therefore, it is particularly critical to gain a full comprehension of the microstructural development mechanisms and the influence of water vapour pressure on the structure and properties of YBCO films.

In this work, we present some experimental data

*Project supported by the National Natural Science Foundation of China (Grant No 50672011) and the Hi-Tech Research and Development Program of China (Grant No 2007AA03Z216).
†Corresponding author. E-mail: dingfz2008@163.com
‡E-mail: guhw@grinm.com

which assign two different steps for the YBCO formation by TFA-MOD. The first step is that the coating is decomposed to oxyfluoride compound and the second step is the growth of the tetragonal YBCO thin film. Moreover, we discuss the influence of water vapour pressure on the microstructure and the critical currents of YBCO films grown on LAO single-crystal substrates in a tubular furnace.

2. Experimental details

The trifluoroacetate precursor solution for YBCO film was prepared by dissolving the acetates of yttrium, barium, and copper in a 1:2:3 cation ratio in de-ionized water with an excess stoichiometric quantity of trifluoroacetic acid at room temperature. The resulting aqueous solution was refluxed for 10 h and then dried to a semisolid state, and then redissolved in methanol for drying. Finally, the residue was dissolved in sufficient methanol to get the final trifluoroacetate precursor solution, whose concentration was 1.5 mol/l. The solution was coated onto 10 mm×10 mm (00h)-oriented LAO substrates at a spinning rate of 3000 rpm for 2 min. Then the samples were put in a quartz tube within a horizontal furnace. Coated films were calcined at the temperature up to 400 °C in 4.2% humidified oxygen with a flow rate of 500 cc/min. The calcined films were fired at 850 °C with different water vapour pressures in humidified Ar gas mixed with 1000 ppm oxygen gas and finally oxygenated at 500 °C for 1.5 h in a pure oxygen gas atmosphere. Different partial water vapour pressures were obtained by bubbling the carrier gas through one gas-washer inside a water bath at different temperatures.

Surface morphologies of YBCO film were observed by field emission scanning electron microscopy (FESEM, FEI-Siron). The phase and texture of the as-grown film was characterized by XRD using Cu-Kα radiation (Philips X' Pert MRD) and Raman analysis. Micro-Raman measurements were carried out using the 5250 Å (1 Å = 0.1 nm) line of an argon-ion laser at room temperature with a Jovin-Yvon T-64000 Raman spectrometer. The laser power on the specimen surface was about 2 mW. The x-ray ω-scan was carried out to evaluate the out-of-plane texture. The in-plane orientations of the film was investigated by means of ϕ-scans. Resistive T_c value was measured by a standard four-probe method and J_c was measured by J_c-scan Leipzig system.[19]

3. Results and discussion

3.1. Intermediate phases

To clarify the intermediate phases after the pyrolysis step, the precursor films coated on the LAO substrate were put in a tubular furnace and heated to 400 °C, 500 °C, 600 °C, 700 °C and 725 °C respectively in 4.2% humidified oxygen mixed with Ar gas. And then the samples were quenched quickly by pulling them out from the furnace to room temperature. The different thermal treatments are illustrated in Fig.1.

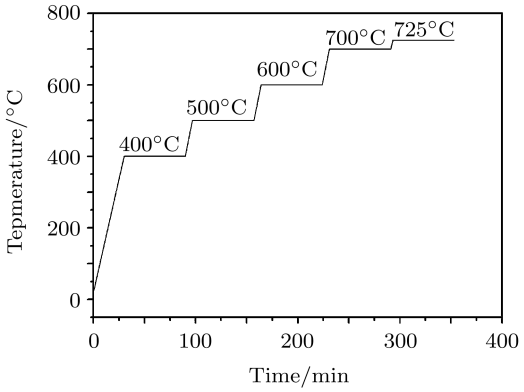


Fig.1. Schematic illustration of the heat-treatment schedule.

Figure 2 shows the XRD patterns of the precursor films heated at 400 °C, 500 °C, 600 °C, 700 °C and 725 °C respectively. All of the reflection peaks in Figs.2(a)–2(d) can be indexed to BaF_2, Y_2O_3 and CuO, respectively. These reflection peaks reveal that the coated film decomposed to BaF_2, Y_2O_3 and CuO at 400–700 °C according to Eq.(1).

$$\mathrm{Y(O_2CCF_3)_3 + Ba(O_2CCF_3) + Cu(O_2CCF_3)_2 + H_2O \xrightarrow{O_2} Y_2O_3 + BaF_2 + CuO + CO_2 \uparrow .} \quad (1)$$

On the other hand, with increasing quenching temperature, the intensities of the intermediate phases get stronger, indicating that the intermediate nanocrystallites grow in size following a coarsening process. Furthermore, it also can be seen from Fig.2(e) that (00l) $YBa_2Cu_3O_{6.5}$ peaks are displaced to at about 725 °C with some second phases, which suggests that the intermediate phases begin to transform into the tetragonal $YBa_2Cu_3O_{6.5}$ according to Eq.(2).

$$\mathrm{BaF_2 + CuO + Y_2O_5 + H_2O \xrightarrow{O_2} YBa_2Cu_3O_{6.5} + HF \uparrow .} \quad (2)$$

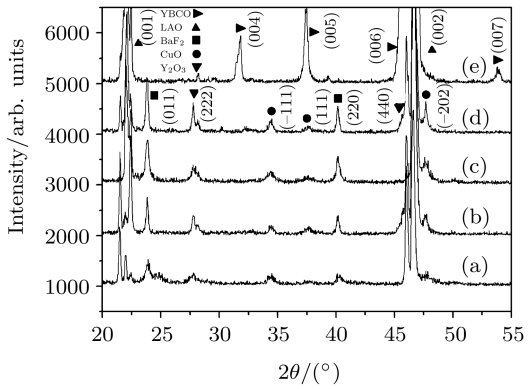


Fig.2. The XRD patterns of YBCO intermediate phases with different quenched temperatures (a) 400 °C, (b) 500 °C, (c) 600 °C, (d) 700 °C, (e) 725 °C.

For further verification, the Raman analysis of the intermediate phases was conducted, as shown in Fig.3. One can see that the Raman spectra display the appearance of the CuO phase as the first crystalline phase (Fig.3(a)) and presence of additional phases BaF_2, which can be clearly identified between 500 and 725 °C (Figs.3(b)–3(e)). We also observe from Fig.3(e) that the tetragonal $YBa_2Cu_3O_{6.5}$ begin formed at 725 °C with BaF_2 and Y_2O_3 phases. The results agree well with the XRD analysis. Thus, the YBCO growth process contains two steps essentially. First, the precursor film begins to be decomposed to BaF_2, Y_2O_3 and CuO at 400 °C, then these nanocrystallites grow in size following a coarsening process between 400 °C and 700 °C. Finally, the intermediate phases transformed into the tetragonal $YBa_2Cu_3O_{6.5}$ at 725 °C.

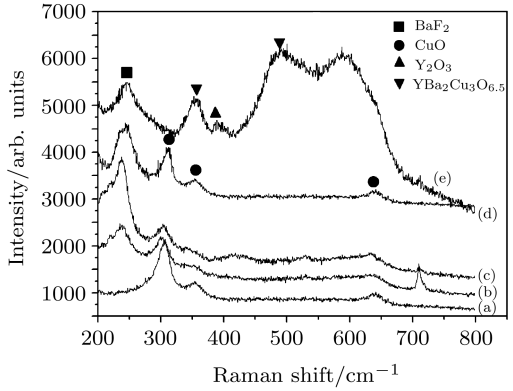


Fig.3. Raman spectra of the YBCO intermediate phases with different quenched temperatures (a) 400 °C, (b) 500 °C, (c) 600 °C, (d) 700 °C, (e) 725 °C.

3.2. Influence of the water vapour pressure

In order to evaluate the effects of the water vapour pressure on the microstructure and critical properties of the YBCO films, we kept all the other processing parameters constant, the firing processes were carried out at different water vapour pressures.

Figure 4 shows the dependence of critical temperature and critical current density on the water vapour pressure for YBCO films. T_c was measured in the range of 89–91 K and the difference between the highest and lowest T_c was 2 K. The results indicated that T_c was not affected much by the water vapour pressure. By contrast, it can be clearly seen that there is a significant change of J_c of the YBCO film depending on the water vapour pressure. In the initial period J_c increased with water vapour pressure. At the water vapour pressure of 40 hPa, the J_c value was only 0.63 MA/cm^2. Maximum J_c value of 3.8 MA/cm^2 was obtained for the YBCO film prepared at water vapour pressure of 190 hPa. With increasing the water vapour pressure, J_c of the YBCO films begins to decrease, which indicates that the films were crystallized fully at water vapour pressure of 190 hPa.

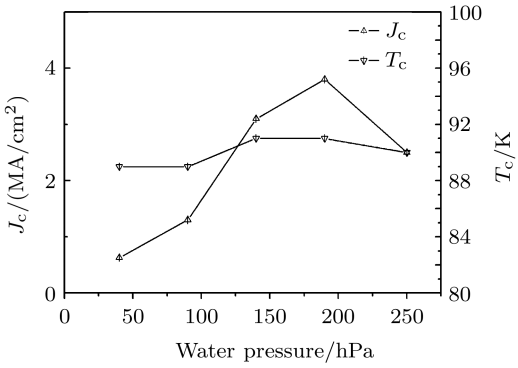


Fig.4. Dependence of T_c and J_c on the water vapour pressure for YBCO films.

Figures 5(a)–5(e) show the XRD patterns of the YBCO films prepared at water vapour pressure of 40 hPa, 90 hPa, 140 hPa, 190 hPa and 240 hPa, respectively. It can be seen that the major diffraction peaks corresponding to the (00l) plane was developed for all the films. But from Fig.5(a), we observe that there are some weak peaks which assigned to BaF_2 impurity phases besides YBCO phase. It suggests that the YBCO film prepared at water vapour pressure of 40 hPa is partially crystallized. Higher resolution XRD patterns with 2θ scaling from 20–25° for the YBCO film is given in right side of Fig.5. For samples a, b and c, there is one peak at 2θ angles of 23.261° which can be indexed to the YBCO (100) phase. It can be concluded that the YBCO a-axis grain is emerged when $P(H_2O)$ is low. On the other hand, the YBCO

films prepared above 190 hPa of water vapour pressure are completely crystallized with a pure YBCO (00l) phase and no impurity phase. Therefore, the $P(H_2O)$ is a key factor to modify the balance between the nucleation rate of *c*-axis and *a*-axis oriented grains at fixed growth temperatures. In our case, the YBCO films prepared with low water vapour pressure (below 140 hPa) have impurity phase and *a*-axis grains. This may be explained as follows: at lower partial water vapour pressure, water molecules consumed to form YBCO thin film are insufficient; when partial water vapour pressure increases until a critical value, water molecules is enough to support pure *c*-oriented YBCO film growth.

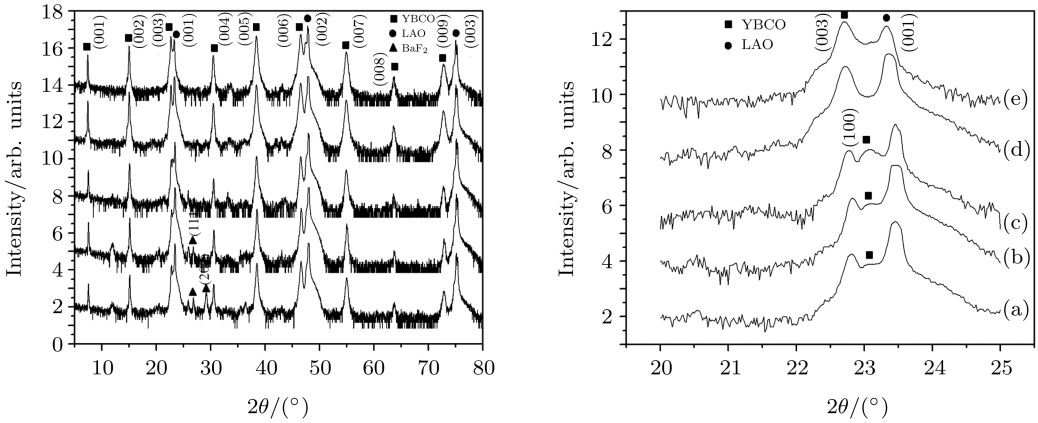


Fig.5. The XRD patterns of YBCO films with different water vapour pressures (a) 40 hPa, (b) 90 hPa, (c) 140 hPa, (d) 190 hPa, (e) 240 hPa.

To characterize the texture of YBCO films, the (1 0 3) phi-scan and x-ray (0 0 5) omega-scan of the YBCO film were performed, as shown in Fig.6. It can be seen that the textures of all of the films were mainly biaxial texture. However, the full width at half maximum (FWHM) of the omega-scans and phi-scans are different. The FWHMs of the out-of-plane texture were measured to be 1.00°, 0.75°, and 0.71° for the films prepared at 140 hPa, 190 hPa, and 240 hPa of water vapour pressure, respectively, and the corresponding FWHMs of the in-plane texture were 0.87°, 0.53°, and 0.51° (as shown in inset of Fig.6). It should to be noted that the YBCO films fabricated above 190 hPa of water vapour pressure show stronger biaxial texture.

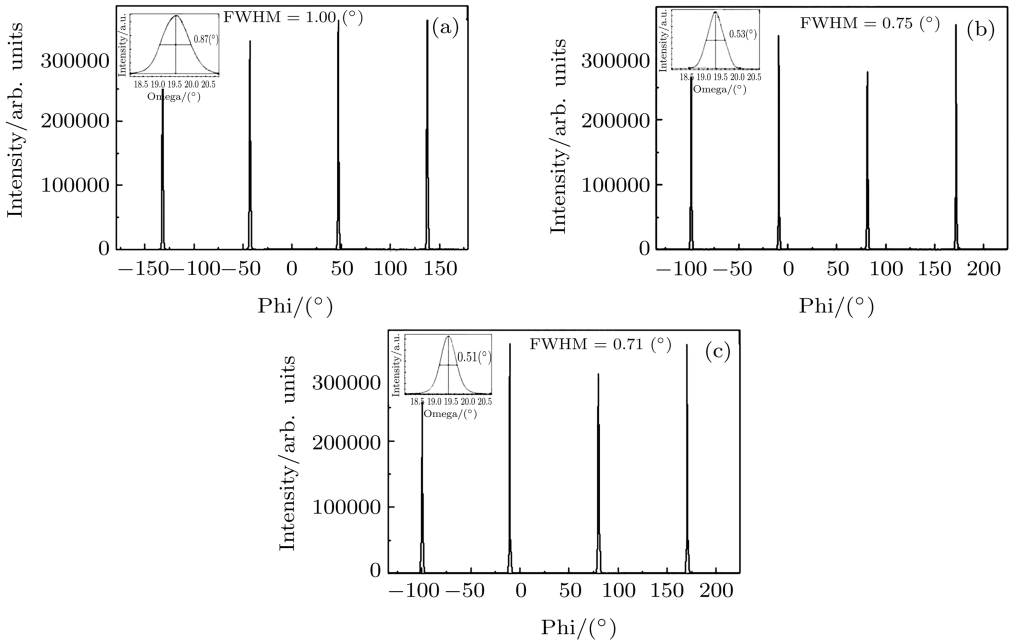


Fig.6. (1 0 3) Phi-scan of the YBCO films prepared at different water vapour pressures (a) 140 hPa, (b) 190 hPa, (c) 240 hPa. The inset shows the (0 0 5) omega-scan of the film.

Figure 7 shows the SEM micrographs of the YBCO thin films prepared at different water vapour pressures. We can observe the evolution of surface morphologies with different water pressures. From Figs.7(a)–7(c), it can be seen that some a-axis grains are easily identified due to their platelet-like shape and their orientation parallel to the orthogonal (100) axes of the substrate. The result is consistent with the XRD analysis. Meanwhile, a smooth surface without any a-axis grain could be observed in the whole area of YBCO film fabricated at 190 hPa of water vapour pressure, which was observed in Fig.6(d). However, when the water vapour pressure increases to 240 hPa, some pores appeared in the YBCO film.

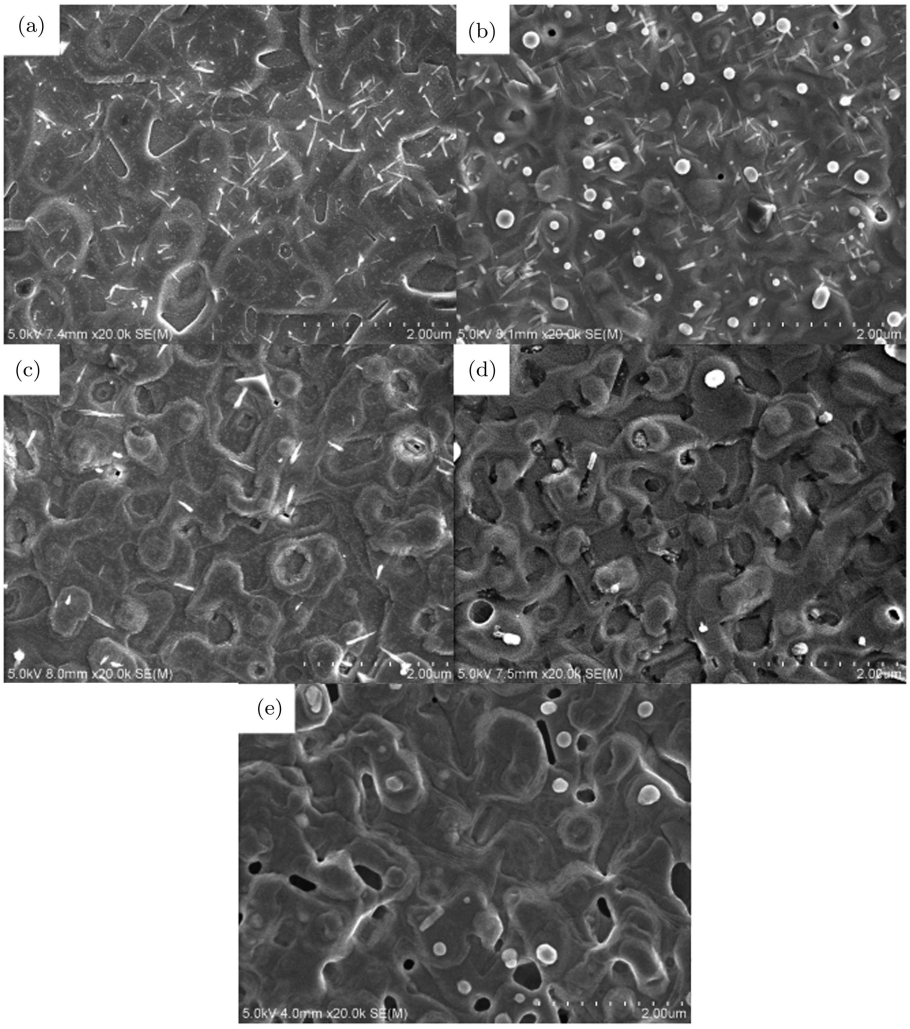


Fig.7. The SEM micrograph of YBCO films with different water vapour pressures (a) 40 hPa, (b) 90 hPa, (c) 140 hPa, (d) 190 hPa, (e) 240 hPa.

Combining with Figs.4, 5 and 6, we can easily find that the critical current density of YBCO film is very sensitive to texture, phase purity and porosity. The YBCO films prepared at low water vapour pressure (40–140 hPa) have lower J_c value due to impurity phases and a-axis grains. The films prepared at 190 hPa of water vapour pressure showed the highest J_c of 3.8 MA/cm^2 which is attributed to the formation of a purer (00l) YBCO phase and stronger biaxial texture.

4. Conclusions

In this study, the reaction mechanism of YBCO growth from TFA precursors was firstly investigated by XRD and Raman analysis. It is indicated that the precursor film has been decomposed to BaF_2,

Y_2O_3 and CuO at 400 °C, then these nanocrystallites grow in size following a coarsening process between 400 °C and 700 °C and finally transform into tetragonal $YBa_2Cu_3O_{6.5}$ at 725 °C. The influence of water vapour pressure on $YBa_2Cu_3O_{7-x}$ film growth on LAO single-crystal substrates was also studied. It is found that $P(H_2O)$ is a key factor to modify the balance between the nucleation rate of *c*-axis and *a*-axis oriented grains at fixed growth temperatures. The films prepared at lower water vapour pressure (40–140 hPa) show poor electrical performance due to *a*-axis grain structure and impurity phases. However, the films prepared at 190 hPa exhibit the highest critical temperature of 90 K and the highest J_c of 3.8 MA/cm^2, which was attributed to the formation of a purer YBCO phase and stronger biaxial texture.

References

[1] Feldmann D M, Ugurlu O, Maiorov B, Stan L, Holesinger T G, Civale L, Foltyn S R and Jia Q X 2007 *Appl. Phys. Lett.* **91** 162501

[2] Haugan T, Barnes P N, Wheeler R, Meisenkothen F and Sumption M 2004 *Nature* **430** 867

[3] MacManus-Driscoll J L, Foltyn S R, Jia Q X, Wang H, Serquis A, Civale L, Maiorov B, Hawley M E, Maley M P and Peterson D E 2004 *Nature Mater.* **3** 439

[4] Endo T, Yoshii K, Iwasaki S, Kohmoto H, Saratani H, Shiomi S, Matsui M and Kurosaki Y 2003 *Supercond. Sci. Technol.* **16** 110

[5] Liu X Z, Tao B W, Deng X W, Zhang Y and Li Y R 2002 *Supercond. Sci. Technol.* **15** 1698

[6] Fabrice A, Dégardin A F and Kreisler A J 2005 *IEEE Trans. Appl. Supercond.* **15** 2907

[7] Gutierrez J, Llordes A, Gazquez J, Gibert M, Roma N, Ricart S, Pomar A, Sandiumenge F, Mestres N, Puig T and Obradors X 2007 *Nature Mater.* **6** 367

[8] Engel S, Thersleff T, Hühne R, Schultz L and Holzapfel B 2007 *Appl. Phys. Lett.* **90** 102505

[9] Araki T and Hirabayashi I 2003 *Supercond. Sci. Technol.* **16** R71

[10] Aoki Y, Teranishi R, Kitoh Y, Fuji H, Nakaoka K, Koyama T, Junko S Matuda, Izumi T, Shiohara Y, Tokunaga Y, Yamada Y, Goto T and Yajima A 2005 *Physica* C **426–431** 945

[11] Zhu Y B, Zhou Y L, Wang S F, Liu Z, Zhang Q, Chen Z H, Lü H B and Yang G Z 2004 *Chin. Phys.* **13** 238

[12] Puig T, Gonzalez J C, Pomar A, Mestres N, Castano O, Coll M, Gazquez J, Sandiumenge F, Pinol S and Obradors X 2005 *Superond. Sci. Technol.* **18** 1141

[13] Hawsey R A and Christen D K 2006 *Physica* C **445-448** 488

[14] Rupich M W, Zhang W, Li X, Kodenkandath T, Verebelyi D T, Schoop U, Thieme C, Teplitsky M, Lynch J, Nguyen N, Siegal E, Scudiere J, Maroni V, Venkataraman K and Miller D 2004 *Physica* C **412-414** 877

[15] Izumi T, Yoshizumi M, Matsuda J, Nakaoka K, Kitoh Y, Sutoh Y, Nakanishi T, Nakai A, Suzuki K, Yamada Y, Yajima A, Saitoh T and Shiohara Y 2007 *Physica* C **463–465** 510

[16] Zhang W, Rupich M W, Schoop U, Verebelyi D T, Thieme C L H, Li X, Kodenkandath T, Huang Y, Siegal E, Buczek D, Carter W, Nguyen N, Schreiber J, Prasova M, Lynch J, Tucker D and Fleshler S 2007 *Physica* C **463-465** 505

[17] Smith J A, Cima M J and Sonnenberg N 1999 *IEEE Trans. Appl. Supercond.* **9** 1531

[18] Wu L, Solovyov V F, Wiesmann H J, Zhu Y and Suenaga M 2002 *Appl. Phys. Lett.* **80** 419

[19] Hochmuth H and Lorenz M 1996 *Physica* C **265** 335